Poly(ethylene oxide)/Poly(dimethylsiloxane) Blend Solid Polymer Electrolyte and Its Dye-Sensitized Solar Cell Applications

Jun Young Lee,[†] Bhaskar Bhattacharya,[†,‡] Dong-Won Kim,[§] and Jung-Ki Park*[,†]

Department of Chemical and Biomolecular Engineering (BK 21 Graduate Program), Korea Advanced Institute of Science and Technology, 373-1 Guseong-dong, Yuseong-gu, Daejeon, 305-701, Republic of Korea, Department of Physics, Hindustan College of Science and Technology, Farah, Mathura 281 122, India, and Department of Chemical Engineering, Hanyang University, Haengdong-dong, Seongdong-gu, Seoul, 133-791, Republic of Korea

Received: April 18, 2008; Revised Manuscript Received: June 2, 2008

Dye-sensitized solar cells (DSSCs) with high efficiency have been fabricated using poly(ethylene oxide)/poly(dimethylsiloxane) blend polymer electrolyte with I^-/I_3^- redox couple in conjunction with a fabricated nanoporous TiO_2 electrode. The blend complexed with LiI has been found to show conductivity close to 10^{-3} S cm^{-1} at 303 K for [EO]:[Li^+] = 20:1. Detailed studies have been reported on the structural and electrical characterization of the polymer electrolyte. The crystallinity modification and the relative number of charge carriers and hence the conductivity have been shown to vary with the PDMS content and also with increasing temperature. The electrolyte dissociation theory has been employed to explain the conductivity behavior. The DSSC with the highest conducting composition of the blend and nanoporous TiO_2 electrode showed 1.35% efficiency at 10 mW cm^{-2}.

1. Introduction

Photoelectrochemical solar cells are of prime interest due to their promising efficiency, cost effectiveness, and ease of fabrication. Several practical problems with the use of liquid electrolytes in such devices, viz., leakage, packaging, evaporation of the liquid, and corrosion of the electrode, can be overcome by replacing the liquid electrolyte with a solid medium. Since the pioneering work by Grätzel,[1,2] dye-sensitized solar cells (DSSCs) based on nanocrystalline TiO_2 electrodes have appeared as a low-cost alternative to the conventional photovoltaic devices. In such solar cells, fluorine-doped tin oxide (FTO) on which a layer of nanoporous TiO_2 coated with a monolayer of dye molecules is brought into contact with the electrolyte. The injection of an electron from the light-induced excited state of the dye molecule into the conduction band of the TiO_2 gives an electron in the outer circuit. The redox reaction in the electrolyte completes the charge transfer loop. For an efficient process, the TiO_2 film is made porous so that the hole-transporting material can penetrate through and a larger surface area be made active. Thus the internal resistance of the cell can be decreased and hence the efficiency will be better. Efforts have been made to use organic hole transport materials,[3] inorganic p-type semiconductors,[4] inorganic fillers,[5] ionic liquids,[6] and various polymer electrolytes.[7] In polymer electrolytes, the conductivity arises from the rapid segmental motion and the interaction between the cation and the donor atom of the main structure. The main focus was made on the modification of poly(ethylene oxide) (PEO) due to its better solvating ability, mechanical stability, and chain flexibility.[8] However, the major drawback of this polymer is its semicrystalline nature at room temperature. It has been established that the amorphous region of the polymer−salt complex provides the conduction pathway and is mainly responsible for the ion conduction in a polymer−salt complex. Therefore, much effort has been directed toward reducing the crystallinity of the polymer (PEO). Different approaches have been made to improve the conductivity of the polymer electrolyte, to make the redox reaction and a swift charge transfer. The major attention was toward the use of plasticizers such as EC and PC.[9] However, this reduction was found to be at the cost of the mechanical strength of the polymer. The uses of different inert fillers for increasing the mechanical strength and the conductivity as well have also been reported.[5] In one of our previous works,[10] we showed the preparation and use of a nanoporous TiO_2 electrode with an ionic liquid modified polymer electrolyte and found an efficiency of 0.63% at 100 mW cm^{-2}.

The other route for the improvement in the above characteristics is to have a structurally modified polymer. The modification is made such that the mechanical stability is retained and the conductivity gets enhanced. The use of polyphospazenes and polysiloxanes, which results in a comblike structure, has been sought as the route for such modifications.[11] Polysiloxanes, with a glass transition temperature of −127 °C, much lower than that of PEO, can enhance the chain flexibility of the oxyethylene chain. As a result, the mobility of the ions should be improved thereby enhancing the conductivity. The PEO as the side chains attached with the siloxane backbone results in the formation of a comblike structure. The high degree of segmental motion in such a structure having the main chain with a polymer of low glass transition temperature will thus result in better conductivity. Similar efforts have been made by a few workers.[12]

In this paper we report the formation of a new blend solid polymer electrolyte, its characterization, and its application in DSSCs. PEO complexed with LiI is modified with poly(dimethylsiloxane) (PDMS). Detailed studies on the effect of varying the PDMS content in the complex at ambient temper-

* To whom correspondence should be addressed. Telephone: 82-42-869-3925. Fax: 82-42-869-3910. E-mail: jungpark@kaist.ac.kr.
† Korea Advanced Institute of Science and Technology.
‡ Hindustan College of Science and Technology.
§ Hanyang University.

10.1021/jp803387k CCC: $40.75
Published on Web 07/23/2008

ature and also with increasing temperature have been reported. A correlation has been established with the number of available charge carriers for the conduction using the electrolyte dissociation theory. A DSSC fabricated using this blend and dye-sensitized nanoporous TiO_2 electrode has also been reported.

2. Experimental Section

2.1. Preparation of Solid Polymer Electrolyte. Poly(ethylene oxide) (PEO, $M_w \sim 5 \times 10^6$, Aldrich), poly(dimethylsiloxane-*co*-methylhydrosiloxane) (PDMS, $M_w \sim 950$, Aldrich), and lithium iodide (LiI, 99.9%, Aldrich) were used as procured. All chemicals were used without further purification. Desired amounts of the polymers and the salt were weighed in a glovebox and dissolved in tetrahydrofuran (THF, Merck). The mixtures were stirred for more than 10 h to ensure the complete complexation of the polymer with the salt. For all samples [EO]:[Li^+] was fixed at 20:1. The PDMS content was varied from 0 to higher weight percent of PEO. The viscous solutions were then cast on glass Petri dishes and dried in an N_2 atmosphere. For complete elimination of the solvent, the films were further dried in a vacuum oven for 2 days at room temperature.

2.2. Characterization of Polymer Electrolyte. The films were subjected to structural, thermal, and electrical characterization for their possible use in electrochemical devices. Fourier transform infrared (FT-IR) spectra were recorded in the attenuated total reflectance (ATR) mode and absorbance mode on a Bruker Tensor 27 spectrometer with the resolution of 4 cm^{-1} in the vibrational frequency range of 600−4000 cm^{-1}.

The surfaces of the films were observed using an optical polarizing microscope (OM, Leica DM LB). Field emission scanning electron microscopy (FE-SEM, FEI Sirion) was also used to observe further details of the surfaces. A differential scanning calorimeter (DuPont TA 2000 DSC) was used to understand the thermal behavior of the blends. Each sample was scanned at a heating rate of 10 °C/min within an appropriate temperature range under a nitrogen atmosphere.

Impedance spectroscopic techniques were used to evaluate the ionic conductivities of the polymer films. The polymer films were sandwiched between two stainless steel (SS) electrodes, and these samples were vacuum-packed in an aluminum plastic pouch to avoid contamination. The ionic conductivities of polymer films were obtained from bulk resistance by ac complex impedance analysis using a Solartron 1455 frequency response analyzer (FRA) over a frequency range of 100 Hz−1 MHz. The conductivity (σ) was calculated from the impedance data, using the relation $\sigma = d/(RA)$, where d and A are the thickness and area of prepared polymer film and R is bulk resistance obtained from the first intercept on the x-axis of the impedance data in the complex plane. The dielectric constant of the blend was evaluated using the impedance data at 1 MHz frequency.

2.3. Fabrication of Cell Assembly. The nanoporous TiO_2 electrodes were fabricated on FTO coated glass substrates. The detailed steps can be seen in our previous report.[10] The FTO (sheet resistance 8 Ω cm^{-2}; Solaronix) coated glasses, cut in 2.5 cm × 2.5 cm samples, were cleaned using an Ultrasonic bath in isopropyl alcohol. A very thin layer of dilute (2 wt % solution in 1-butanol) titanium (IV) bis(acetylacetato)diisopropoxide (Merck) was spin coated over the FTO and then sintered at 300 °C. This thin layer works as a blocking layer that reduces the losses due recombination between the holes (or cations in electrolytes) and the electrons in the FTO. Thus the dark currents of the devices decrease considerably. The nanosized TiO_2 layer was obtained over it by doctor blading the TiO_2 paste (Ti-Nanoxide HT, Solaronix). The thickness of this layer was controlled by Scotch tape. The film was first dried in room temperature and then sintered at 500 °C. A dye, *cis*-bis(isothiocyanato)bis(2,2′-bipyridyl-4,4′-dicarboxylato)ruthenium(II) (Solaronix), generally called N3, was used as a sensitizer. Finally, for sensitizing with dye, the above electrode was immersed in a 3×10^{-4} mol dm^{-3} ethanol solution of dye for 24 h. A Pt counter electrode (CE) was prepared by spin coating H_2PtCl_6 solution (Aldrich, 0.05 mol dm^{-3} in isopropyl alcohol) onto the FTO conductive glass and then sintering it at 400 °C for 30 min.

For incorporation of the I^-/I_3^- redox couple in the electrolyte, extra iodine (Aldrich, 10 wt % of LiI salt) was added to the highest conducting composition of the polymeric solution. This polymer electrolyte was, then, dropped over the dye-soaked electrode using a dropper. The platinum coated FTO glass plate, used as the counter electrode, was placed over the polymer and

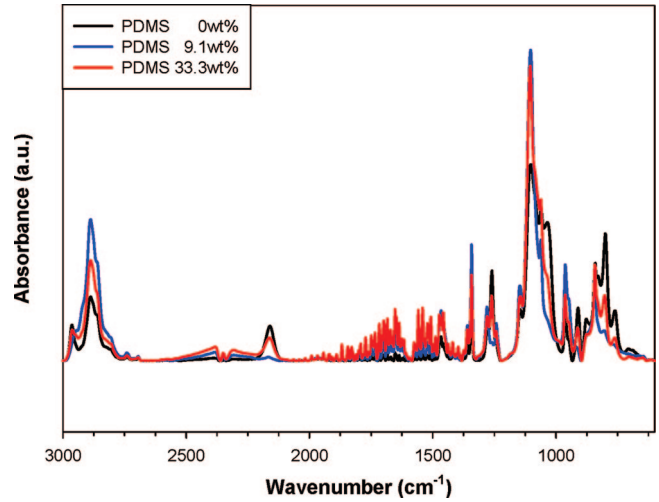

Figure 1. FT-IR absorption spectra of polymer blend films.

TABLE 1: Some Important IR Peaks and Their Respective Assignments[a]

peak positions (cm^{-1})			
pure PEO	pure polysiloxane	salt−polymer complex	assignments
2940−2790		2940−2790	CH_2 stretching (asymmetric and symmetric)
	~2860	2858	CH_3 symmetric stretching
	2156	2156	CO stretching (weak)
1960		1967	PEO (overtone)
	1925	1923	Si−CH overtone
1466		1465	CH_2 bending (asymmetric)
1450		1450	CH_2 bending
	1410−1390	1410−1390	CH_2 in plane
1356		1359	CH_2 wagging/CC stretching
1342		1342	CH_2 wagging (asymmetric)
1280		1278	CH_2 twisting
		1259	
1240		1233	CH_2 twisting
1147		1150	CC stretching/COC stretching
	~1100	1103−1105	asymmetric Si−O−C
	1100−1000	1100−1000	Si−C stretching, "$-(SiO)_n-$"
	1085	1083	Si−O stretching
958		962	COC stretching
948		945	CH_2 rocking/COC stretching
		908	
	870	877	Si-CH_3 rocking
844		842	CH_2 rocking
	840	840	Si−C stretching end group
	~800	798	Si−C stretching, "$-(SiO)_n-$"

[a] The positions of pure PEO and PDMS are also listed along with the observed peaks of the final complex.

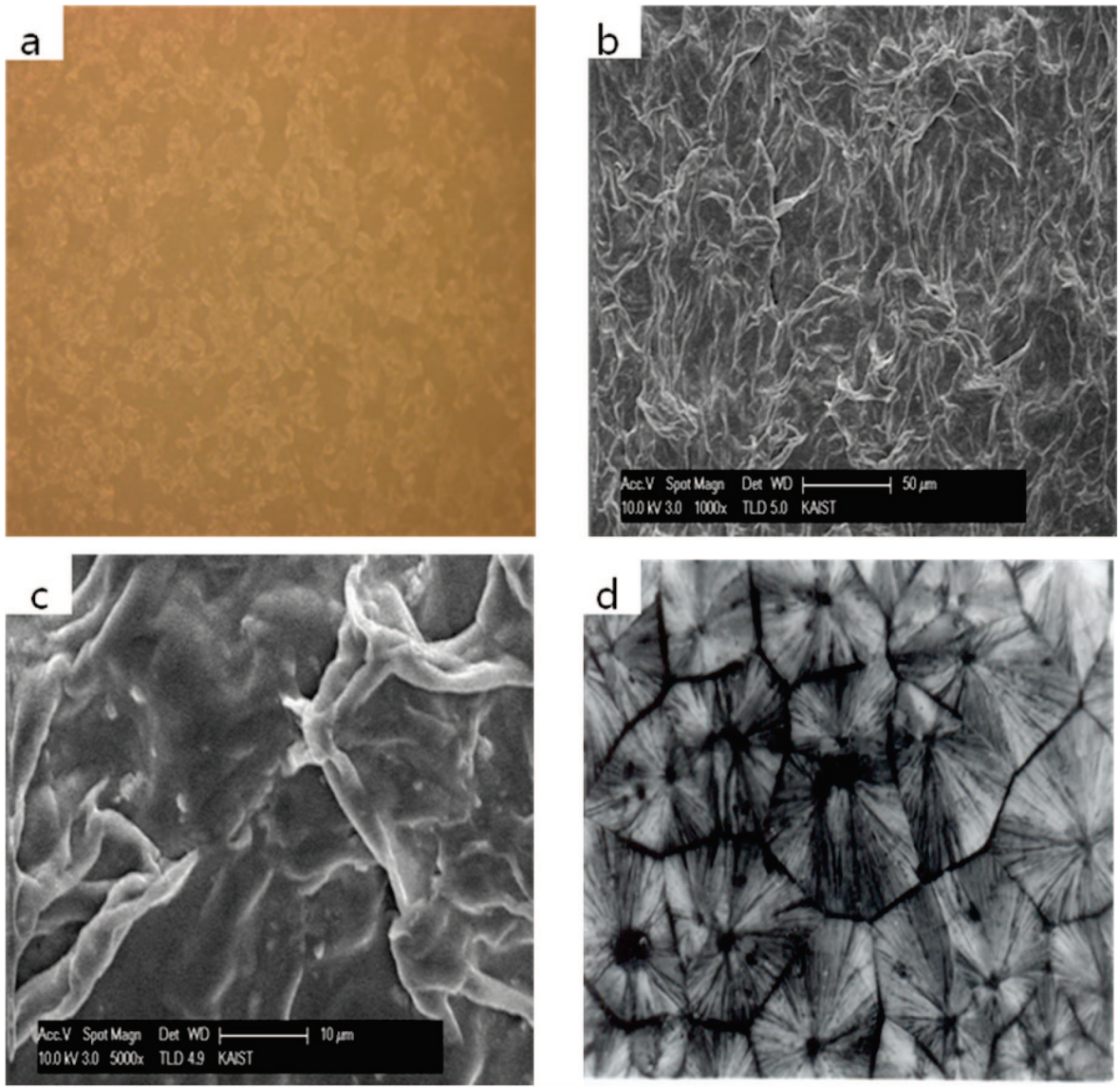

Figure 2. Surface morphology of polymer films. (a) under polarizing microscope at ×500; (b, c) SEM showing foldlike irregularities; (d) large spherulites.[16]

the assembly was left for drying without any further sealing. The photovoltaic tests of the DSSCs were carried out by measuring the current−voltage ($J-V$) characteristics under illuminations of 100 and 10 mW cm^{-2}.

3. Results and Discussion

3.1. FT-IR Analysis. All polymer films were subjected to infrared spectroscopic studies. Figure 1 shows the spectra of the PEO/PDMS blend polymer films for different PDMS concentrations. Peaks corresponding to various vibrational modes of the two polymers were observed in the spectra. No additional peak, other than from the constituent polymers, was observed in the spectra. Since the basic structure of either polymer can result in many possible modes of CH_2, all corresponding peaks were reflected in the spectra.[13] The intensities of the peaks were found to increase with the addition of PDMS in PEO. This increase is directly related to the number of available bonds performing the corresponding mode of vibration. The conformations of pure PEO and its alkali metal salt complexes have been studied extensively by many workers using vibrational spectroscopy.[14] Pure PEO has trans, T(CC−OC); trans, T(CO−CC); gauche, G(OCCO); and T2G conformations. The presence of bands at ∼958, 948, and 844 cm^{-1} corresponding to the CH_2 symmetrical and asymmetrical rocking of pure PEO shows the presence of the gauche conformation of $O-[(CH_2)_2]-O$. Generally, the coordination of alkali metal ions with PEO does not affect the gauche conformation of PEO. Besides, the asymmetric peak due to C−O−C stretching confirms the hanging of the Li^+-I^- with the ether oxygen in the chain of PEO. Similar results have been observed by many workers and used for ascertaining the complexation of the salt with the polymer.[15] Table 1 shows some of the important bands observed in the spectra along with their possible conformations.

3.2. Morphology. The morphologies of the polymer films were observed under an optical microscope (OM) and a scanning electron microscope (SEM) as well. Figure 2a−c shows the optical micrograph and SEM photographs of the film. No special feature is observed in the micrograph or under SEM. The regular spherulitic structure[16] of the PEO:LiI complex (Figure 2d) is found to be absent in the polymer films containing PDMS. The absence of the spherulites indicates the decrease in the crystallinity of the polymer matrix. Under the SEM, the surface of

TABLE 2: Glass Transition Temperatures (T_g), Melting Peak Positions of Crystalline PEO and the Crystalline Complex of PEO, Corresponding Changes in Enthalpy, and Relative Crystallinities of the Samples

		peak position (°C)			
system	T_g (°C)	T1	T2	ΔH_m (J/g)	crystallinity
PEO	−67	68			77
PEO:LiI		56	68	109.8	58.4
(PEO + 9.1 wt % PDMS) + LiI	−45.2	50	61	56.6	23.2
(PEO + 16.7 wt % PDMS) + LiI	−46.5	53	62	57.8	23.6
(PEO + 23.1 wt % PDMS) + LiI	−44.2	52	63	73.1	30
(PEO + 28.6 wt % PDMS) + LiI	−45.3	49	57	33.8	13.8
(PEO + 33.3 wt % PDMS) + LiI	−43.6	54	62	47.3	19.3
(PEO + 50 wt % PDMS) + LiI	−43.6	53	−	73.3	30

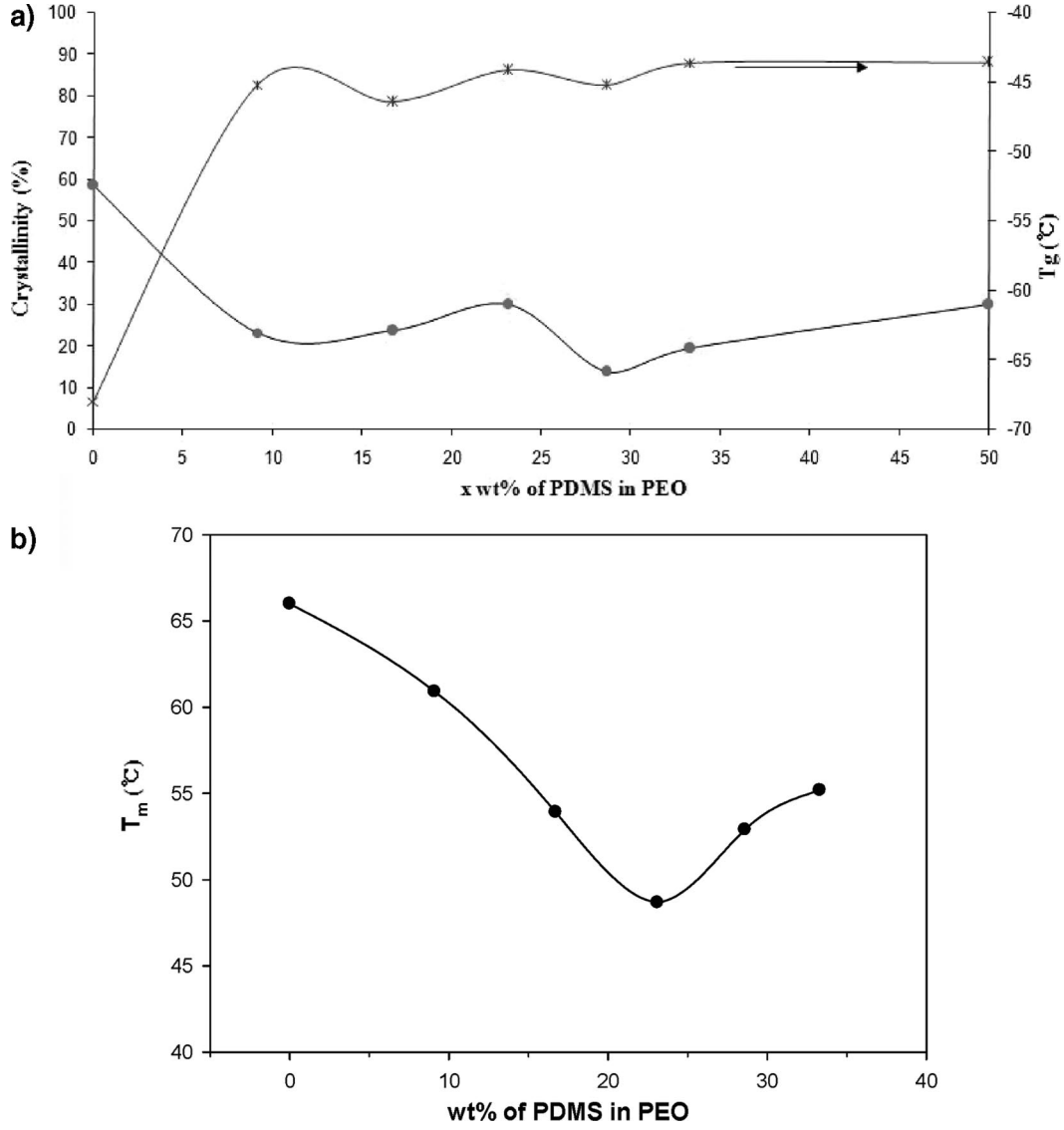

Figure 3. (a) Variation in glass transition temperature (−∗−∗−) and relative percentage crystallinity (−●−●−) of films with increasing PDMS content. (b) Change in softening temperature (T_m) with addition of PDMS.

the films appeared as having many "fold"-like wavy structures which are completely random and rough. Such roughness is supposed to be good for better adhesion with the electrodes in the devices.[5b]

3.3. Analysis of Thermal Properties. Differential scanning calorimetric studies have been carried out on the samples. The curves show two step changes which are attributed to the glass transition temperature T_g and melting (or softening) temperature T_m of the blend. The presence of only one T_g in the thermograph confirms the formation of the PEO−PDMS blend and its structural compatibility. Further, it is known that the glass transition temperature in polymeric systems is associated with segmental motion of the polymer chains. The addition of a plasticizer is known to change the T_g and hence modify the segmental motion. In our systems the T_g increases significantly on addition of PDMS in PEO. The T_g values are listed in Table 2 and plotted against the composition in Figure 3a. After the initial increase, though, T_g values does not change much with increasing PDMS content in PEO but the variation matches that of the change in enthalpy at melting. The softening temperature

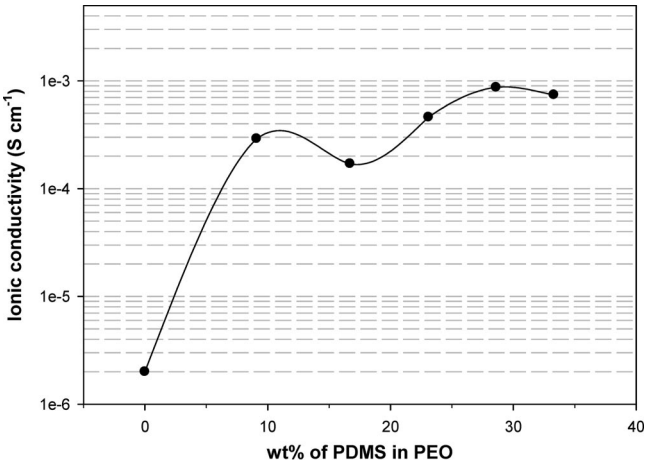

Figure 4. Ionic conductivity at 303 K of PEO:PDMS blends.

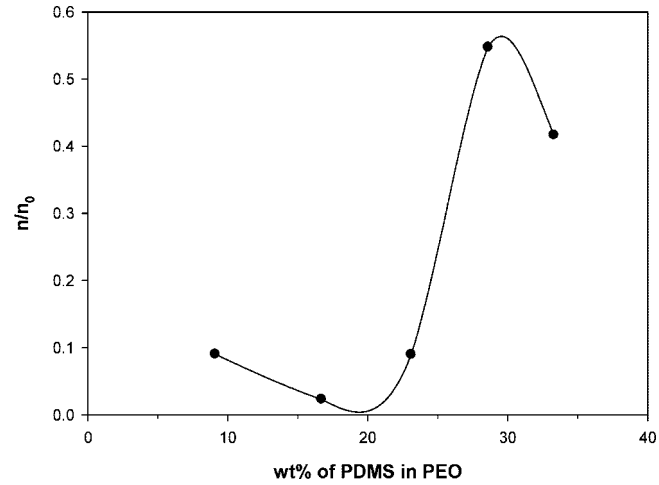

Figure 5. Change in relative number of charge carriers with increasing amount of PDMS in the blend.

(the combined peak) slightly decreases due to addition of PDMS up to 23.1 wt % and then becomes almost constant. The decrease in the T_m is due to the fact that PDMS is liquid at room temperature (viscosity $\sim$ 900 Pa s) and can work as a plasticizer for the semicrystalline PEO. The plot showing variation in T_m with weight percentage of PDMS is shown in Figure 3b. The samples showed clear melting of the matrix. From the peaks we could identify the two partially overlapped peaks. The two peaks are attributed to the melting of the crystalline parts of the host polymer PEO and the crystalline polymer salt complex. The peak positions (geometrically deconvoluted) are listed in Table 2. The area under the melting curve is directly related to the crystallinity (or to the change in enthalpy in the melting). Therefore, knowing the area one can calculate the crystallinity of the sample. Since geometrically deconvoluted peaks and measurement of their respective area may involve errors, we have used the total change in the enthalpy in the melting of total crystalline parts. Assuming pure PEO to be 100% crystalline, for which the change in enthalpy $\Delta H_m = 45$ cal/g,[17] the relative crystallinities of all the samples were obtained by approximating the values of the change in enthalpy, ΔH_m, corresponding to the combined melting of PEO crystalline peak and the peak due to the complex. The values of ΔH_m and the relative crystallinity are also listed in Table 2. A plot showing the variation in crystallinity with the variation in composition (i.e., x) is given in Figure 3a. The relative crystallinity is found to decrease until almost 25% due to the addition of PDMS. The increase, though small, in the crystallinity on addition of more than 30 wt % PDMS may be due to the possible segregation of PDMS from PEO. The consequence of the changes in crystallinity has been discussed in the following section.

3.4. Conductivity as a Function of PEO/PDMS Ratio. Figure 4 shows the conductivity with the varying concentration of the PDMS at 303 K. As mentioned above, the [EO]:[Li^+] was kept fixed for all the samples. It is observed that the conductivity increases by more than 2 orders of magnitude on addition of 10 wt % of PDMS in PEO. The conductivity further passes through a small dip and then increases to its maximum of $<10^{-3}$ S cm^{-1} (to be more precise, 8.7×10^{-4} S cm^{-1}). The variation in the conductivity is explained in terms of the change in the relative crystallinity of the polymer−salt complex. The composition variation of conductivity is found to be correlated with the variation of crystallinity given earlier. The conductivity drops when the crystallinity is more and vice versa. A direct correlation can be seen from Figure 4. Though it was possible to obtain good films even with 100 wt % of PDMS, we could notice the segregation of the PDMS from the film starting from 60 wt % of PDMS. Therefore, we have not discussed the conductivity and other properties beyond 50 wt % of PDMS in PEO.

As explained by Sato,[18] for glassy electrolytes, the conductivity depends upon the percolation efficiency, which is a measure of degree of deviation of ionic motion from the ideal random walk. In other words, it is the effectiveness of ionic motion toward making long-distance diffusion. In the ordered state, the percolation efficiency decreases, thereby decreasing the conductivity. The addition of PDMS reduces the crystallinity of the total system drastically, and hence the conductivity increases. The small decrease in conductivity near 16 wt % is attributed to the ion association effect.[19] It may be noted that, after the initial decrease in the crystallinity, it increases slightly up to 25 wt %. This increase could have resulted in the decrease of the total conductivity. However, at the same time, we found that the number of free charge carriers (discussed below) increases almost 7 times its value at 10 wt % PDMS (Figure 5). This behavior can be attributed to the redissociation of the undissociated salt and the breaking of higher charge multiplates with the increase in the chain flexibility due to the addition of PDMS in the complex medium. Beyond its blending limit, the crystallinity shows an increasing trend which results in the stabilization of the conductivity values. This statement is also supported by the number of charge carriers as shown in Figure 5. At the blending limit ($\sim$30 wt %), the n/n_0 is maximum and then shows a decreasing trend. The conductivity, therefore, in this PEO:PDMS blend system is predominantly governed by the number of charge carriers. The addition of PDMS results in the change in the dielectric constant of the matrix which results in the change in the number of free charge carriers and thereby the conductivity.

3.5. Conductivity as a Function of Temperature. The change in conductivity was studied with temperature, and the result is shown in Figure 6. The conductivity increases rapidly, indicating an Arrhenius type thermally activated process. This pattern can be expressed as

$$\sigma = \sigma_0 \exp\left\{\frac{-E_a}{kT}\right\}$$

where σ_0 is the preexponential factor and E_a is the activation energy required for the process. The estimated values of the preexponential factor (σ_0) and the activation energy (E_a) from the postmelting region of the curve are 4.7×10^{-3} and 0.73

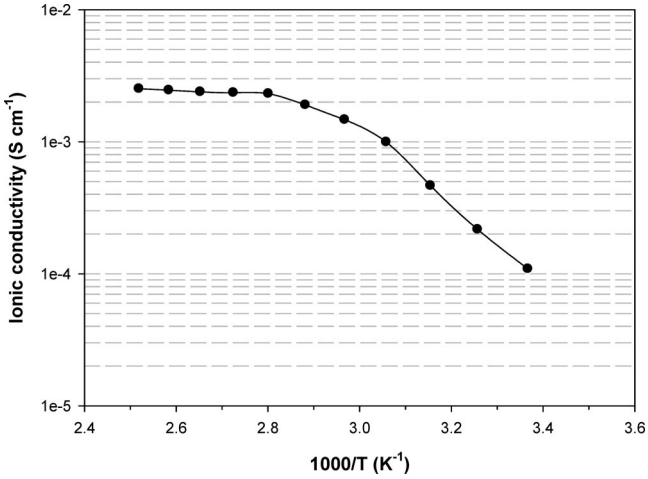

Figure 6. Change in conductivity with temperature reflecting the melting of the crystalline regions of the polymer and its complex.

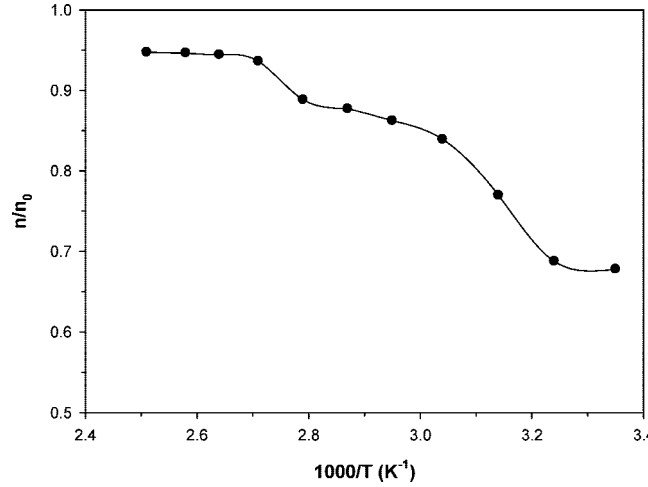

Figure 7. Variation in the relative number of free charge carriers on heating.

eV. The increase can be attributed to the melting of the crystalline part of the PEO and its complex and thus a sharp jump showing the crystalline to amorphous phase transition. The initial slope of the curve slightly decreases after 55° and then attains a plateau. The change in slope can be attributed to the two different but nearby melting temperatures of the crystalline part of the polymer and its crystalline complex with the salt. Similar reports reflecting the two step melting can be seen in the literature.[15] This region is well reflected in the dielectric constant and has been discussed in the following section in terms of the change in the number of free charge carriers.

3.6. Number of Charge Carriers. We know that the conductivity (σ) of the material is equal to the product ($nq\mu$) of the charge carrier density n, the charge of the carrier q, and its mobility μ. Therefore any increase in either of the parameters n or μ will result in the increase in the conductivity σ. In order to estimate the contribution of the number of free charge carriers in the total conductivity, the dielectric constant of the film was calculated at 1 MHz frequency. The electrolyte dissociation theory of Barker[20] was employed, and by use of the following relation the relative change in the carrier concentration was calculated.

$$n = n_0 \exp\left\{\frac{-U}{2\varepsilon kT}\right\}$$

Here U stands for the dissociation energy of the salt, k is the Boltzmann constant, and ε is the dielectric constant of the system at temperature T. We have calculated the relative number of charge carriers (n/n_0) for our samples at room temperature and also at different temperatures. The consequences due to the variation in n/n_0 with composition have been discussed in section 3.4. The plot of n/n_0 with temperature is shown in Figure 7. From the figure we can see that (the slope of the curve) the relative concentration of charge carriers increases rapidly with increase in temperature, and then crossing a plateau increases further and attains a constant value. This behavior can be directly correlated with the conductivity behavior with increasing temperature. The initial increase can be attributed to the melting of the crystalline regions of the PEO and thereby allowing more charge carriers to participate in the conduction. It may be noted that the amorphous region of the polymer (and the polymer−salt complex) is responsible for the charge conduction and has been established by the free volume measurement of similar systems.[21] Thus the local melting will result in the availability of more carriers and therefore increase in the conductivity. Similarly, the second rise in the conductivity and the n/n_0 can be attributed to the melting of the crystalline complex. These temperatures showing an increase in σ can be matched with the DSC data showing the melting of the crystalline part of the polymer and its complex.

3.7. Photovoltaic Performance. The highest composition of the blend was used as the electrolyte in the DSSC. The $J-V$ characteristics in the dark and under white light illumination at 100 mW cm^{-2} are shown in Figure 8a. The total reaction at the Pt electrode/electrolyte interface can be described as

$$3I^- \leftrightarrow I^{3-} + 2e^-$$

The $J-V$ characteristics in the dark indicated typical Schottky type behavior, confirming the formation of the junction and respective barrier. In the dark, there is almost no current, until the contacts start to inject heavily due to forward biasing larger than the open circuit voltage. The S-shape of the curve indicates the formation of an energy barrier at the electron collecting anode. Under illumination, the contribution due to photogenerated charge carriers is reflected. At the short circuit condition the maximum generated photocurrent could be seen, whereas at the flat-band condition the photogenerated current is balanced to zero. Between these two points the maximum power point is identified and the corresponding efficiency is calculated. The V_{OC} has been found to be 0.54 V and J_{SC} is 3.05 mW cm^{-2} at 100 mW cm^{-2}, and they are 0.48 V and 0.66 mW cm^{-2} respectively at 10 mW cm^{-2}. The solar cell regions of the characteristics are shown in Figure 8b. The DSSC parameters calculated from the $J-V$ plots under illumination are listed in Table 3. The better response observed at 10 mW cm^{-2} indicates better charge generation and collection at the electrodes. It may be noted that both the V_{OC} and J_{SC} decrease with decreasing intensity of the light. This decrease in V_{OC} has been attributed to the decrease in the band bending under pinned Fermi level condition.[22] The change in J_{SC} is directly related to the number of photogenerated minority carriers, which is obviously less at less intensity (low photon flux).[23] The efficiency of the cells was found to be much better than those reported using only PEO as the polymer electrolyte, where the efficiency is only ~0.01%.[5a] This behavior can be compared with those using PEO/KI (+I_2) with ionic liquid reported by us earlier, where it reaches 0.63%. This improvement in the cell properties is attributed to the increase in the conductivity of the polymer

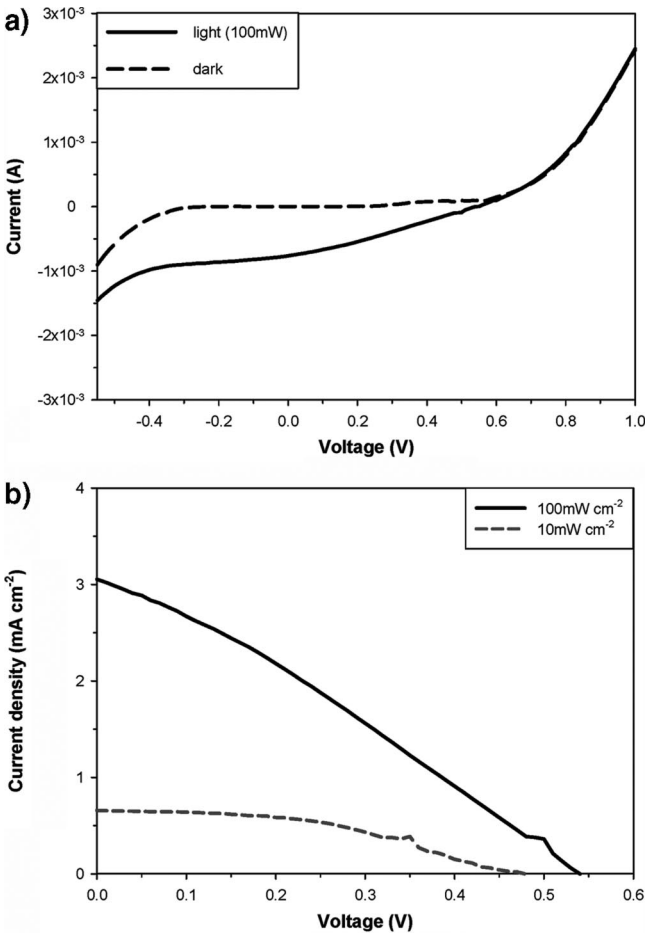

Figure 8. (a) Current−voltage characteristics of DSSC fabricated using the new blend in the dark and under white light illumination at 100 mW cm^{-2}. (b) Solar cell region of the cell used for evaluation of cell parameters and efficiency (—, 100 mW cm^{-2} illumination; ---, 10 mW cm^{-2} illumination).

TABLE 3: Cell Parameters Obtained from the *J*−*V* Characteristics of the Cells[a]

intensity (100 mW cm^{-2})	J_{SC} (mA cm^{-2})	V_{OC} (V)	FF	η (%)
PEO + PDMS:LiI + I_2	3.05	0.54	0.29	0.48
PEO + PDMS:LiI + I_2, at 10 mW cm^{-2}	0.66	0.48	0.43	1.35
PEO:KI + I_2	0.06	0.68	0.26	0.01 (a)
PEO + KI + IL + I_2	1.89	0.65	0.52	0.63 (b)

[a] The data corresponding to (a) and (b) are taken from refs 5a and 10.

electrolyte due to the presence of PDMS as discussed in preceding sections. It may be noted that the room temperature during the measurement was ∼15 °C and the relative humidity was only ∼20%. Any increase in either of the two parameters may also result in further enhancement in the conductivity of the blend and therefore the efficiency of the cells.

4. Conclusions

PEO/PDMS blend complexed with LiI was found to show conductivity close to 10^{-3} S cm^{-1} at 303 K. The addition of PDMS in PEO reduces the crystallinity of the matrix. The conductivity is found to depend more on the number of charge carriers. The dye-sensitized solar cells fabricated using the nanoporous TiO_2 electrode and the solid polymer blend showed photoconversion efficiencies of 0.48% and 1.35% at 100 and 10 mW cm^{-2}, respectively.

Acknowledgment. This work was supported by the Brain Korea 21 (BK 21) project under the Ministry of Education, Science and Technology, Republic of Korea.

References and Notes

(1) (a) O'Regan, B.; Grätzel, M. *Nature* **1991**, *353*, 737. (b) Nazeeruddin, M. K.; Kay, A.; Rodicio, I.; Humphry-Baker, R.; Mueller, E.; Liska, P.; Vlachopoulos, N.; Grätzel, M. *J. Am. Chem. Soc.* **1993**, *115*, 6382.

(2) Grätzel, M. *J. Photochem. Photobiol., C: Photochem. Rev.* **2003**, *4*, 145.

(3) Cervini, R.; Cheng, Y.; Simon, G. *J. Phys. D: Appl. Phys.* **2004**, *37*, 13.

(4) (a) Tennakone, K.; Kumara, G. R. R. A.; Wijayantha, K. G. A. *Semicond. Sci. Technol.* **1996**, *11*, 1737. (b) Meng, Q.-B.; Takahashi, K.; Zhang, X.-T.; Sutanto, I.; Rao, T. N.; Sato, O.; Fujishima, A. *Langmuir* **2003**, *19*, 3572.

(5) (a) Kang, M. S.; Kim, J. H.; Kim, Y. J.; Won, J.; Park, N. G.; Kang, Y. S. *Chem. Commun.* **2005**, 889. (b) Stergiopoulos, T.; Arabbtzis, I. M.; Katsaros, G.; Falaras, P. *Nano Lett.* **2002**, *2*, 1259.

(6) (a) Dai, Q.; Menzies, D. B.; Macfarlane, D. R.; Batten, S. R.; Forsyth, S.; Spiccia, L.; Cheng, Y.; Forsyth, M. *C. R. Chim.* **2006**, *9*, 617. (b) Fei, Z.; Kuang, D.; Zhao, D.; Klein, C.; Ang, W. H.; Zakeeruddin, S. M.; Grätzel, M.; Dyson, P. J. *Inorg. Chem.* **2006**, *45*, 10407. (c) Stathatos, E.; Lianos, P.; Jovanovski, V.; Orel, B. *J. Photochem. Photobiol., A: Chem.* **2005**, *169*, 57.

(7) (a) Nogueira, A. F.; De Paoli, M.-A.; Montanari, I.; Monkhouse, R.; Nelson, J.; Durrant, J. R. *J. Phys. Chem. B* **2001**, *105*, 7517. (b) Nogueira, A. F.; Durrant, J. R.; De Paoli, M.-A. *Adv. Mater.* **2001**, *13*, 826.

(8) MacCallum, J. R.; Vincent, C. A. *Polymer electrolyte reviews 1 & 2*; Elsevier: New York, 1989.

(9) (a) Chatzivasiloglou, E.; Stergiopoulos, T.; Kontos, A. G.; Alexis, N.; Prodromidis, M.; Falaras, P. *J. Photochem. Photobiol., A: Chem.* **2007**, *192*, 49. (b) Nelles, G.; Rosselli, S.; Miteva, T.; Yasuda, A.; Tsvetanov, C. Patent Number EP1840152, 2007. (c) Noguira, V. C.; Longo, C.; Nogueira, A. F.; Soto-Oviedo, M. A.; De Paoli, M.-A. *J. Photochem. Photobiol., A: Chem.* **2006**, *181*, 226.

(10) Bhattacharya, B.; Tomar, S. K.; Park, J.-K. *Nanotechnology* **2007**, *18*, 485711.

(11) (a) Blonsky, P. M.; Shriver, D. F. *J. Am. Chem. Soc.* **1984**, *106*, 6854. (b) Bannister, D. J.; Doyle, M.; Macfarlane, D. R. *J. Polym. Sci.* **1985**, *23*, 465.

(12) (a) Splinder, R.; Shriver, D. F. *Macromolecules* **1988**, *21*, 648. (b) Albinsson, I.; Mellander, B.-E.; Stevens, J. R. *Polymer* **1991**, *32*, 2712. (c) Kunde, N.; Paulmer, R. D. A.; Shyamala, S.; Khosla, N. K.; Kulkarni, A. R. *J. Mater. Sci. Lett.* **1995**, *14*, 271. (d) Watanabe, M.; Nagano, S.; Sanui, K.; Ogata, N. *J. Power Sources* **1987**, *20*, 327. (e) Zhou, G.; Khan, I. M.; Smid, J. *Macromolecules* **1993**, *26*, 2202. (f) Wintersgill, M. C.; Fontanella, J. J.; Smith, M. K.; Greenbaum, S. G.; Adamic, K. J.; Andeen, C. G. *Polymer* **1987**, *28*, 633.

(13) Socrates, G. *Infrared and Raman Characteristic Group Frequencies*, 3rd ed.; John Wiley & Sons, Ltd.: New York, 2005.

(14) Papke, B. L.; Ratner, M. A.; Shriver, D. F. *J. Electrochem. Soc.* **1982**, *129*, 1434.

(15) (a) Maurya, K. K.; Srivastava, N.; Hashmi, S. A.; Chandra, S. *J. Mater. Sci.* **1992**, *27*, 6357. (b) Srivastava, N.; Chandra, S. *Phys. Status Solidi A* **1997**, *163*, 313.

(16) Hashmi, S. A.; Kumar, A.; Maurya, K. K.; Chandra, S. *J. Phys. D: Appl. Phys.* **1990**, *23*, 1307.

(17) Griffin, L. O. *Physical Constants of Linear Homopolymers*; Springer: Berlin, 1986.

(18) Sato, H. *Solid State Ionics* **1988**, *28/30*, 333.

(19) Noda, A.; Hayamizu, K.; Watanabe, M. *J. Phys. Chem. B* **2001**, *105*, 4603.

(20) Barker, R. E., Jr.; Thomas, C. R. *J. Appl. Phys.* **1964**, *35*, 3203.

(21) Halder, B.; Singru, R. M.; Maurya, K. K.; Chandra, S. *Phys. Rev.* **1996**, *B54*, 7143.

(22) Snaith, H. J.; Grätzel, M. *Adv. Mater.* **2006**, *18*, 1910.

(23) Snaith, H. J.; Grätzel, M. *Adv. Mater.* **2007**, *19*, 3643.

JP803387K